Numerical simulation of the temperature evolution in a room with a *mur neutralisant.* Application to "The City of Refuge" by Le Corbusier.

C. Ramírez-Balas[a], E. D. Fernández-Nieto[b], G. Narbona-Reina[b], J. J. Sendra[a], R. Suárez[a]

[a]*Instituto Universitario de Arquitectura y Ciencias de la Construcción. Escuela Técnica Superior de Arquitectura. Universidad de Sevilla. Av. Reina Mercedes 2. 41012 Sevilla, España*
[b]*Departamento de Matemática Aplicada I. Escuela Técnica Superior de Arquitectura. Universidad de Sevilla. Av. Reina Mercedes 2. 41012 Sevilla, España*

Abstract

This paper examines a mathematical model of the thermal evolution in a specific room of "The City of Refuge", built in Paris (1933) by Le Corbusier. Although the architect proposed an environmental conditioning system by combining two technological advances: the *mur neutralisant* −a double-glazed wall with an air cavity that can be heated or cooled− and the *respiration exacte* −a purified circulating air maintained at constant temperature−, this was never incorporated. This article aims to acquire knowledge of indoor air distribution in the room under study by considering the combination of the *mur neutralisant* and the *respiration exacte.*

The problem is resolved through a "coupled code". The first is a two-dimensional model simulating the temperature evolution in the room, while the second is a one-dimensional model used to represent the problem of the *mur neutralisant.* The numerical model develops the technical issues associated with the implementation of computational fluid dynamics (CFD).

The numerical simulations carried out validate the solution of the system proposed. Control of the façade temperature using the active chamber ensures that the operative temperatures obtained for summer and winter fall within the comfort range. The City of Refuge is the clearest precursor of modern active façade systems.

Keywords: *Mur neutralisant*, *respiration exacte*, Le Corbusier, The City of Refuge, Active façade system, Double Skin Façade (DSF), Computational Fluid Dynamics (CFD), Numerical simulation.

1. Introduction

The case study analyses the atmosphere of the City of Refuge in Paris (1929-30), an experimental building in which Le Corbusier attempted to implement two of his own discoveries, the

mur neutralisant and the *respiration exacte*, to support his concept of *machine à habiter* and to show the adaptation of new glass architecture to environmental conditions. The combined use of these two elements aimed to maintain indoor comfort temperature and ideal indoor air quality conditions throughout the year, regardless of outdoor environmental conditions.

To do so, the large glazed south façade would be composed of the *mur neutralisant*, with double sheets of glass and an active air chamber, into which air was to be introduced in order to maintain a constant indoor temperature regardless of the season (Figure 1(a)). *Respiration exacte*, a ventilation system completely independent from this wall while acting in conjunction with it, would guarantee a suitable indoor air quality in the building, and would contribute to the indoor thermal quality of rooms with a *mur neutralisant* (Figure 1(b)) [12].
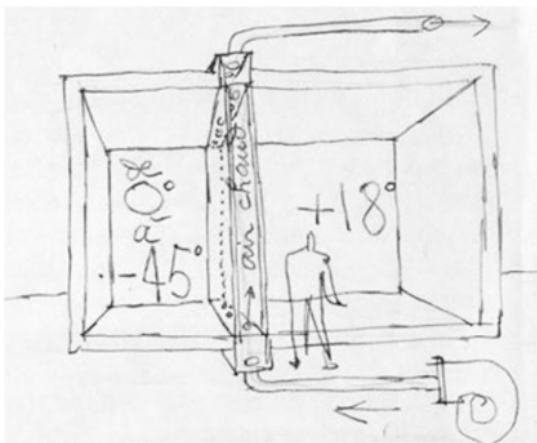
(a) Description of the *mur neutralisant*.
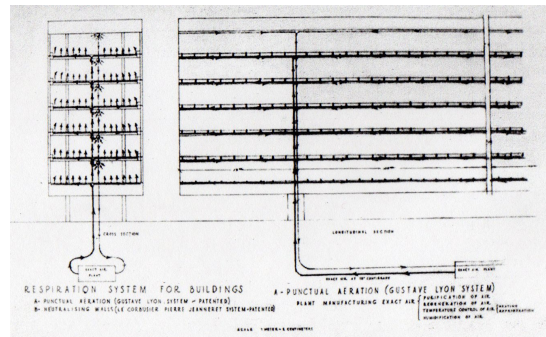
(b) Schematic drawing of the *respiration exacte*.

Figure 1: Sketches by Le Corbusier about The City of Refuge.

The City of Refuge, belonging to the Salvation Army, was a building designed for the homeless [25]. It could house up to 600 people, distributed in large dormitories and "roomettes", small rooms used mainly for single women with children. For the City of Refuge to be more than a mere shelter for the night it required installations on several levels that could operate throughout the day, meeting the needs of its occupants [11].

The building was placed in an urban context, but practically isolated from other buildings. It is composed of a basement floor, for workshops, laundry rooms and machine rooms; the "pilotis" floor, used for workshops, kitchens and conference rooms; and the ground floor, used for access (see Figure 2). The *mur neutralisant* was meant to be executed between the first and fifth floors, acting as the envelope for the female dormitories −the first floor case study− as well as for the

smaller rooms between the second and fifth floors [3].

Respiration exacte was finally installed in the City of Refuge in Paris, but not so the *mur neutralisant*, which was never incorporated for financial reasons and technical concerns. It was replaced with a *pan de verre* similar in appearance to the *mur neutralisant*, but with quite different thermal behaviour, creating the need for a traditional heating system installation, although the building lacked a cooling system. This makes it impossible to establish its behaviour as an environmental conditioning solution in relation to the building façade, either alone or in combination with the *respiration exacte*.

Although the construction of the *mur neutralisant* had been ruled out, Le Corbusier reserved the space for its construction and maintained an interest in the results it would have produced had it been executed. This interest led engineers from the Saint Gobain company to resume trials in August 1932, when the *pan de verre* had already been installed in the City of Refuge.
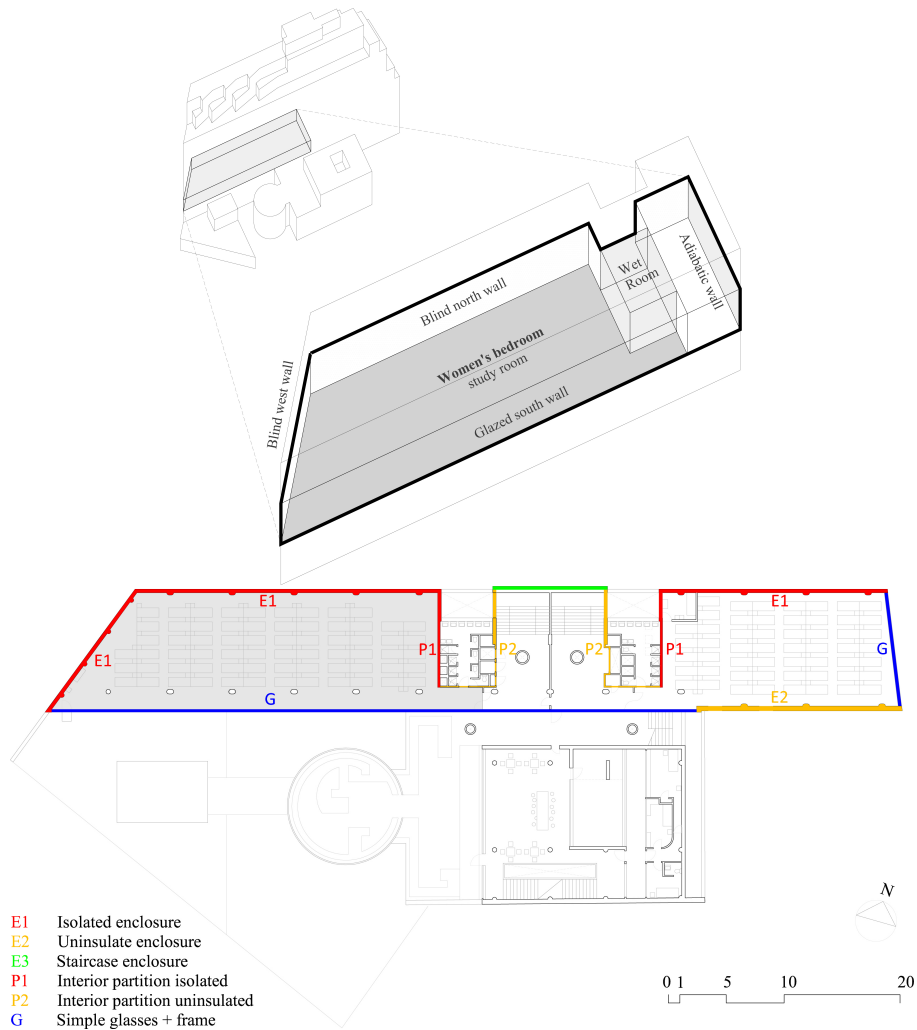
Figure 2: Situation of the case study in the City of Refuge and detail of the first floor.

Several tests were carried out on different types of glazing in order to verify the coefficients for heat transmission proposed by G. Lyon, and to check the operation of the air heating system of the active chamber [22].

These trials provided the heat transmission coefficients for different types of glazing: 2 mm, 7 mm and 12 mm double glazing with a 100 mm active chamber.

The following conclusions were reached from the result of the trials [19]:

- A maximum impulse flow of 60 l/s was to be ensured.

- The maximum width of the active chamber should be set at 100 mm, since at greater widths the convection currents would cause a reduction in heat exchange and an increase in thermal loss.

- A thermal difference of at least 10°C should be maintained between the airflow to the exterior from the chamber and the indoor temperature of the heated room, in order to compensate for

thermal loss.

This research aims to resolve the physical problems resulting from the combination of the *mur neutralisant* and the *respiration exacte* and establish what the real system behaviour would have been if both these innovations had been implemented in the City of Refuge as planned by Le Corbusier and calculated by G. Lyon (Figure 1(b)).

The *mur neutralisant* is composed of a 7 mm double glass sheet with an active inner chamber measuring 100 mm, through which hot or cold air was circulated depending on the time of the year in order to provide active thermal isolation (see Figure 1(a)). This system is extremely difficult to model and simulate. In fact, current energy and environmental computer simulation programs, such as DesignBuilder [6], cannot be used for this system, especially not combined with Le Corbusier's mechanical ventilation system, *respiration exacte*. Therefore `FreeFem++` software (v. -3.20) was chosen [10]. This program uses C++ language to process and calculate all sorts of mathematical codes and solution methods for assessment with Computational Fluid Dynamics (CFD). Specific models and programs were created for this study using algorithms integrating all phenomena and physical characteristics in order to reproduce the combination of both of Le Corbusier's systems for the City of Refuge.

The energy models generated take into account climate conditions in Paris, profiles of usage and operating conditions, and the spatial and material characteristics of the envelope of the City of Refuge. This made it possible to calculate the main parameters of the thermal environments of the room studied and to carry out graphic representations of the evolution of interior climate in relation to variations in exterior climate: differences in temperature, airflows, thermal radiation, etc. In short, simulation using `FreeFem++` codes makes it possible to reliably predict what the interior temperature of the spaces designed would be.

Given the interest in the progress and development of energy efficiency systems and energy preservation in buildings, double skin façades (DSF) are currently a major research topic as studies of Joe et al. [18] and Ghadimi et al. [13]. In [24], Shameri et al. analyse different elements relating to the design of DSFs, such as geometrical characteristics, types of glass, natural lighting, wind loads, etc. Ventilation and solar protection systems are the most important systems in the inner chamber of the double skin given the reduction in thermal gain produced through the envelope.

Zhou et al. [27] present the main methods for the analysis of the thermal behaviour of DSFs, developed to prevent overheating, mainly for cold climate zones in winter and warm climates

in summer. The application of ventilated DSFs with an integrated and controlled solar protection device makes it possible to control the building's thermal conditions in these sorts of climates.

Research by Chen et al. [5] uses a mathematical model for a glass double skin façade with slats in the inner air chamber to reduce solar gains in climates with warm summers.

At present, models and simulation using programmed software are some of the most powerful tools available for research on thermal behaviour and fluid dynamics in ventilated DSFs, known as Active Transparent façades (ATFs), as one of three different façade analyzed through 3d Computational Fluid Dynamics (CFD) in the study of Brandl et al. [4]. For example, Ismail et al. present a two-dimensional model with numerical simulation of heat transfer in single glazing [15]. This model is based on an energy equation applying the terms of absorbed, transmitted and reflected solar radiation, as well as exterior and interior convection flows through the glass, depending on the incident solar radiation and outdoor temperature. This initial research serves as an introduction to the problem and was subsequently developed by the same authors [16], paying special attention to the effects of mass flow in the chamber between the double glazing in order to determine the superficial temperature of the inside glass. They establish how the increase in mass flow of the natural ventilation reduces total heat gain in comparison with a single glazed window. Research by Ismail et al. [17] was taken into consideration when establishing the mathematical model for the *mur neutralisant* case study. These authors describe a transitory two-dimensional model formulated using basic mass and energy conservation equations associated with variations in climate and atmospheric conditions. Thus, the results are obtained for the temperatures along and through the air chamber with mechanical ventilation. This study examines a numerical method different to that proposed by Ismail et al. [17] or Liu et al. [20], discretising the equation into partial differentials which define the model for studying the evolution of temperature in the *mur neutralisant*. These calculations also take into consideration the coupling of the *mur neutralisant* and the evolution of indoor temperatures.

This article has mainly been prompted by the lack of research focusing jointly on the simulation of the *mur neutralisant* and *respiration exacte*. The implementation and subsequent simulation using `FreeFem++` entails two main tasks. The first is the coupling of a 1D and 2D model. Physical problems and solution methods are applied to the problem of *respiration exacte* (2D model), a code for an implicit resolution of the problem of the *mur neutralisant* (1D model) and finally, a coupled code for the correct operation of the combination of *mur neutralisant* and *respiration exacte*. The second task is the definition of the mathematical codes in the 1D model, since an implicit method of finite volumes should be established as a resolution procedure, in order to

optimize simulation time for the problems of the *mur neutralisant* with respect to the problem of *respiration exacte* (2D model) with minimum margin of error in the solutions.

2. Coupled model for the temperature evolution problem

This section defines the mathematical model proposed to solve the temperature evolution problem. The main objective is to assess the influence of the *mur neutralisant* on the temperature of the room with the *respiration exacte* system. As mentioned above, the problem is divided into two physical systems: the *mur neutralisant* is examined using a 1D problem, while a 2D problem is used to evaluate the indoor temperature.

Figure 3 shows a diagram of the operation of the coupled problem. Thus, in order to establish a final time t_f, it is necessary to first solve the 2D problem and obtain the indoor temperature, T_{int}. This data is then used to resolve the 1D problem, calculating the temperature of the internal glass, T_{ig}, which is embedded into the 2D problem as a boundary condition.
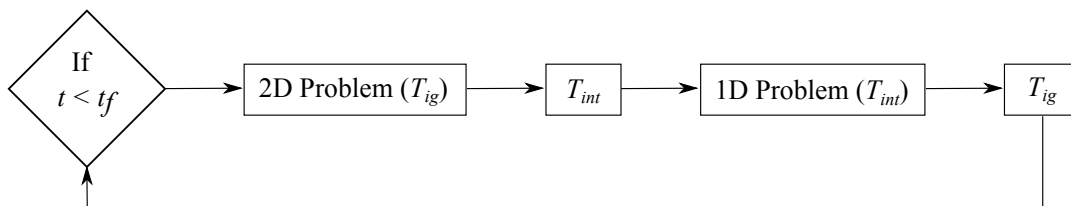

Figure 3: Diagram of the operation of the coupled 1D - 2D problems.

In order to give a complete graphic description of the whole domain we show in Figure 4 the schematic representation of the studied room (2D problem) and a cross section of the *mur neutralisant* (1D problem). In the following subsections we detail the numerical approximations of the 1D and 2D models.
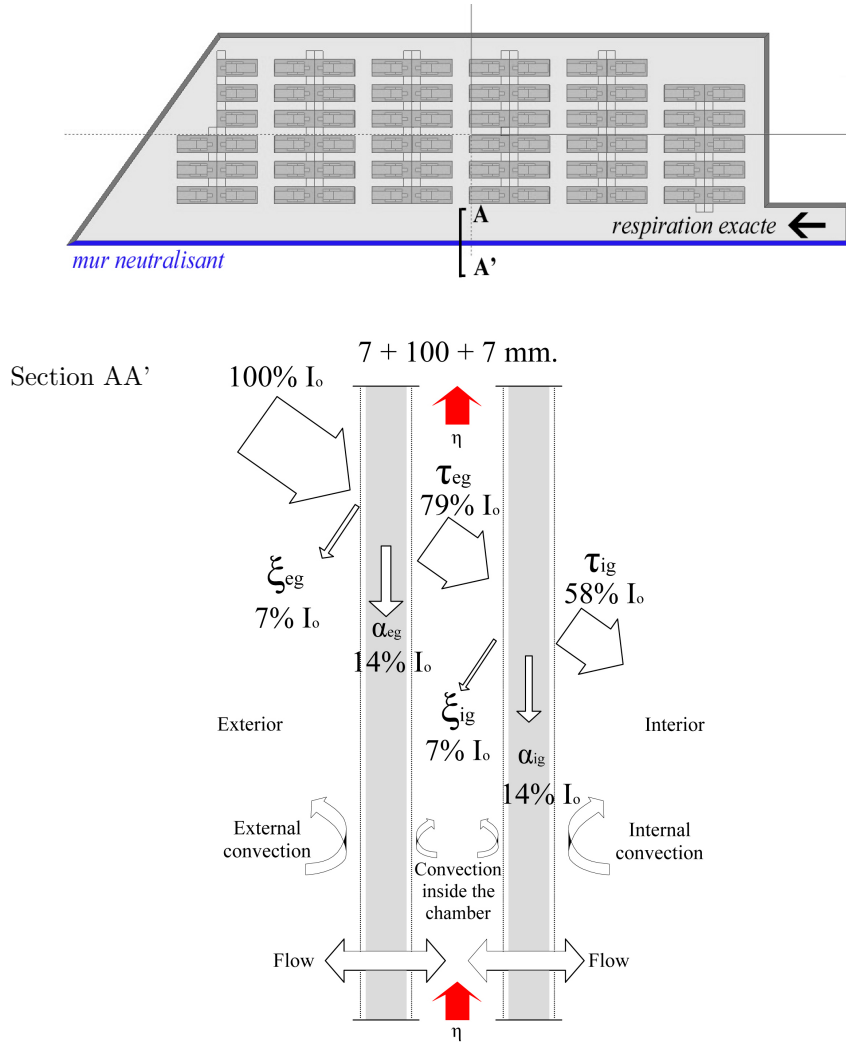
Figure 4: Complete physical domain and detail of physical phenomena in the *mur neutralisant*.

2.1. Evolution of indoor temperature (2D problem)

Temperature evolution is simulated using a convection-diffusion problem. Since the room is affected by a *respiration exacte* system, it is necessary to first calculate the velocity field to be used by the convection phenomena. This problem is modelled on the Navier-Stokes equations, and the unknowns are the velocity field (solution of the Navier-Stokes problem) and the temperature (solution of the convection-diffusion problem). The density is assumed to be constant and the fluid is incompressible. Here we consider a study domain Ω with boundaries Γ_i $(i = 1, \ldots, M)$. We assume that the initial glass wall is located on the boundary Γ_1 and the entrance of the *respiration exacte* is made through the boundary Γ_3, the rest of the boundaries are assumed to be internal walls. For the case of the City of Refuge the schedule of the domain Ω is shown in Figure 4, the

corresponding boundaries are represented in Figure 7. The system required is written as

$$
\begin{cases}
\dfrac{\partial \vec{u}}{\partial t} + \vec{u} \cdot \nabla - \nabla \cdot (\nu \nabla \vec{u}) + \nabla q = \vec{g} & \text{in } \Omega \\[2mm]
\nabla \cdot \vec{u} = 0 & \text{in } \Omega \\[2mm]
\dfrac{\partial T}{\partial t} + \vec{u} \cdot \nabla T - k \Delta T = \varphi & \text{in } \Omega \\[2mm]
T = T_{ig1d(m)} & \text{on } \Gamma_1 \\[2mm]
T = T_{extef} & \text{on } \Gamma_3 \\[2mm]
T = T_{rad} & \text{on } \Gamma_2 \cup \Gamma_4 \cup \ldots \cup \Gamma_M
\end{cases}
\tag{1}
$$

with initial condition

$$
T(0) = T_{op} \qquad \text{in } \Omega.
$$

where:

$\vec{u}$: Velocity field,

T : Temperature,

t : Time,

$\nu = \frac{\mu}{\rho}$: Kinematic viscosity,

$q = \frac{p}{\rho}$: Pressure,

$\vec{g} = \frac{\vec{f}}{\rho}$: Density of the heating source due to the radiation,

k : Thermal diffusion coefficient.

φ : Source term due to the occupancy.

The different notations for boundary conditions are as follows: $T_{ig1d(m)}$ is the temperature of the internal glass wall, imposed on the boundary Γ_1. This value is obtained by averaging the temperature obtained by the 1D problem on the internal glass. T_{rad} is the heating temperature of the walls enclosing the room. These walls are labelled $\Gamma_2, \Gamma_4, \ldots, \Gamma_M$, with $(M-1)$ being the number of boundaries considered in the internal walls (see Figure 7). Thus, it is possible to impose different heating temperatures in each of them. The boundary Γ_3 is used to simulate the entrance of the *respiration exacte*, so T_{extef} is the temperature of this incoming flow. Finally, T_{op} is the initial temperature assumed for the room over the domain Ω.

The numerical approximation of this problem was carried out using the mixed $\mathbb{P}_2 - \mathbb{P}_1$ Finite Element method. FreeFem++ software was used for the computing implementation.

2.2. Simulation of the mur neutralisant (1D problem)

2.2.1. The mur neutralisant

The solution proposed, though not incorporated, by Le Corbusier was that of a double plane of glass with air recirculation in the inner chamber heated/cooled by the building's air conditioning system to provide greater thermal insulation than that provided by openings with single glazing or with double glazing and passive air chambers. Controlling the temperature of the interior air

9

of the chamber would depend on exterior climate conditions for each day and hour of study. The problem is considered as a system consisting of two sheets of glass, 7 mm thick and 2.8 m long (L), separated by a width W = 0.10 m, forming an active air chamber with a constant temperature. Below is a detailed description of the phenomena and parameters which affect the increase in temperature and are caused mainly by the incidence of solar radiation on the glazed façade. For this purpose, solar radiation was considered as the sum of the amount of solar energy directly received, both diffused and reflected, together with convection and airflow phenomena (Figure 4).

Finally, the upper and lower parts of the ends of the glazing were considered adiabatic, since Le Corbusier planned to prolong the construction of the *mur neutralisant* from the first to the fifth floor. Thus, we analyse a floor of height 2.8 m as a part of the complete 5 m wall where the *mur neutralist* is installed (see [16]). The conditions for the ends in contact with the indoor and outdoor environments were obtained through the energy balance carried out in the DesignBuilder simulation [6].

The different forms of heat transfer considered were taken into account in the formulation of the problem using the data for the glass used in this study. The outer pane receives 100% of the incident solar radiation, 7% of which is reflected to the exterior environment, with 14% being absorbed by the outer pane. The remaining 79% of energy incides on the interior glass, where 7% is transmitted to the chamber through reflection and 14% is absorbed by the inner pane. Therefore, the total energy transmission to the interior environment is 58% of the incident solar radiation. In addition, the convection phenomenon is considered a result of heating the panes of glass in surfaces in contact with the exterior and interior, as well as in surfaces in contact with the air chamber.

2.2.2. Mathematical model and numerical approximation

The problem involves the temperature of the three parts of the *mur neutralisant*. T_f denotes the temperature of the fluid inside the wall cavity, while T_{eg} and T_{ig} represent the temperatures of the external and internal glass respectively. The problem is then solved by the following system of partial differential equations:

$$\begin{cases} (\rho c V)_f \dfrac{\partial T_f}{\partial t} = -\eta c \dfrac{\partial T_f}{\partial z} + U_c A(T_{eg} - T_f) + U_c A(T_{ig} - T_f) \\[4mm] (\rho c V)_{eg} \dfrac{\partial T_{eg}}{\partial t} = U_{ext} A(T_{ext} - T_{eg}) + U_c A(T_{f,i} - T_{eg}) + \sigma \varepsilon_{eg}(T_{ext}^4 - T_{eg,i}^4) + \alpha_{eg} I_o + Q_{eg} \\[4mm] (\rho c V)_{ig} \dfrac{\partial T_{ig}}{\partial t} = U_{int} A(T_{int} - T_{ig}) + U_c A(T_f - T_{ig}) + \sigma \varepsilon_{ig}(T_{int}^4 - T_{ig}^4) + \alpha_{ig} \tau_{eg} I_o + Q_{ig} \end{cases} \quad (2)$$

with $z \in [0, L]$, L being the length of the *mur neutralisant* and $t \in [t_0, t_M]$ the time (see specific notation in Appendix B).

The previous model (2) can be represented as a system of equations under the time derivative of the three temperatures of the fluid, internal and external glass as follows:

$$\begin{cases} \partial_t T_f = g_f(t, T_f, T_{eg}, T_{ig}), & t \in [t_0, t_M] \quad z \in [0, L] \\ \partial_t T_{eg} = g_{eg}(t, T_f, T_{eg}, T_{ig}) \\ \partial_t T_{ig} = g_{ig}(t, T_f, T_{eg}, T_{ig}) \end{cases}$$

where

$$\begin{cases} g_f(t, T_f, T_{eg}, T_{ig}) = -\eta c \frac{\partial T_f}{\partial z} + U_c A(T_{eg} - T_f) + U_c A(T_{ig} - T_f) \\ \\ g_{eg}(t, T_f, T_{eg}, T_{ig}) = U_{ext} A(T_{ext} - T_{eg}) + U_c A(T_f - T_{eg}) + \sigma \varepsilon_{eg}(T_{ext}^4 - T_{eg,i}^4) + \alpha_{eg} I_o + Q_{eg} \\ \\ g_{ig}(t, T_f, T_{eg}, T_{ig}) = U_{int} A(T_{int} - T_{ig}) + U_c A(T_f - T_{ig}) + \sigma \varepsilon_{ig}(T_{int}^4 - T_{ig}^4) + \alpha_{ig} \tau_{eg} I_o + Q_{ig} \end{cases}$$
$$(3)$$

The unknowns of the problem are functions in time and space,

$$T_f = T_t(t, z), \quad T_{eg} = T_{eg}(t, z), \quad T_{ig} = T_{ig}(t, z).$$

Thus, the numerical approximation begins by defining a partition of the independent variables t and z.

- A uniform partition of the interval $[t_0, t_M]$ with $M + 1$ points is considered. That is, M subintervals of length $\Delta t = \frac{t_M - t_0}{M}$, so the partition is defined as

$$t_k = t_0 + k\Delta t, \quad k = 0, 1, \ldots, M.$$

- A uniform partition of the space interval $[0, L]$ given by the points is considered

$$z_{i+1/2} = i\Delta z, \quad i = 0, \ldots, n,$$

  n being the number of subintervals composing $[0, L]$, that is, $\Delta z = \frac{L}{n}$.

A semi-implicit Euler method in time and a Finite Volume Approximation for the space variable are considered to solve the system. Thus,

$$\{(T_{f,i}^k, T_{eg,i}^k(z), T_{ig,i}^k(z))\}, \quad \begin{matrix} k = 0, \ldots, M, \\ i = 1, \ldots, n, \end{matrix}$$

the approximated unknowns in time t_k in the control volume $[z_{i-1/2}, z_{i+1/2}]$. That is,

$$T_{f,i}^k \approx \frac{1}{\Delta z} \int_{z_{i-1/2}}^{z_{i+1/2}} T_f(t_k, z) dz.$$

When the Finite Volume method is applied, the temperature of the fluid inside the wall cavity at the interface point $z_{i+1/2}$ is approximated $T^{k+1}_{f,i+1/2}$. Taking into account that the air flow is rising, an upwind method is used to approximate it by $T^{k+1}_{f,i}$.

The evolution in time is then combined with this space approximation by using the semi-implicit Euler method. The solution is obtained from the following system:

$$
\begin{cases}
T^{k+1}_{f,i} = T^k_f + \Delta t \, g^{k,k+1}_{f,i} \\[2ex]
T^{k+1}_{eg,i} = T^k_{eg} + \Delta t \, g^k_{eg,i} \\[2ex]
T^{k+1}_{ig,i} = T^k_{ig,i} + \Delta t \, g^k_{ig}
\end{cases}
$$

where:

$$
g^{k,k+1}_{f,i} = -\eta c \frac{T^{k+1}_{f,i} - T^{k+1}_{f,i-1}}{\Delta z} + U_c A (T^k_{eg,i} - T^k_{f,i}) + U_c A (T^k_{ig,i} - T^k_{f,i}),
$$

$$
g^k_{eg,i} = U_{ext} A (T^k_{ext,i} - T^k_{eg,i}) + U_c A (T^k_{f,i} - T^k_{eg,i}) + \sigma \varepsilon_{eg} ((T^k_{ext,i})^4 - (T^k_{eg,i})^4) + \alpha_{eg} I^k_o + Q^k_{eg,i},
$$

$$
g^k_{ig,i} = U_{int} A (T^k_{ind} - T^k_{ig,i}) + U_c A (T^k_{f,i} - T^k_{ig,i}) + \sigma \varepsilon_{ig} ((T^k_{ind})^4 - (T^k_{ig,i})^4) + \alpha_{ig} \tau_{eg} I^k_o + Q^k_{ig,i}.
$$

Furthermore, it must be taken into account that for the first space subinterval the boundary condition is the temperature of the entrance air into the wall cavity. This is the value of $T^{k+1}_{f,0}$. The net heating radiation transference calculation, $Q_{ig,i}$ and $Q_{eg,i}$, is specified in the following subsection.

2.2.3. Radiation method

This section presents the radiation method used to determine the net heating radiation transfer, $Q_{ig,i}$ and $Q_{eg,i}$, for one of the surfaces with respect to the other surfaces of the wall cavity. The energy balance for a surface i with area A_i is described as:

$$
\frac{Q_i}{A_i} = J_i - G_i \tag{4}
$$

where J_i is the radiation energy ratio that leaves the surface and G_i is the irradiation ratio received by the surface. These are determined as follows:

• G_i, the irradiation ratio received, is calculated as the sum of the form-factor F_{ij} between the point z_i of the external glass and the point z_j of the internal glass:

$$
G_i = \sum_{j=1}^n F_{ij}, \tag{5}
$$

• The form-factor for two parallel sheets of glass, F_{ij}, can be deduced through the phenomena represented in Figure 5 leading to the expression (6),
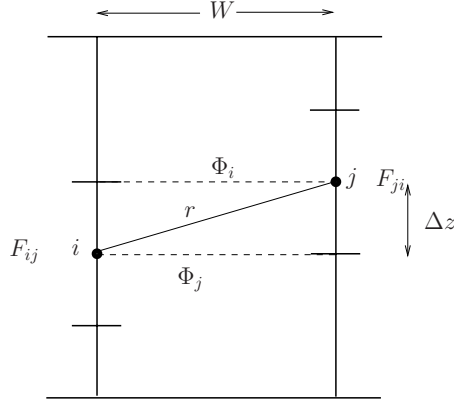
Figure 5: Form-factor between the two parallel sheets of glass of the *mur neutralisant*.

$$F_{ij} = \frac{1}{A_i} \int_{A_i} \int_{A_j} \frac{\cos\phi_i \cos\phi_j}{\pi r^2} dA_j dA_i, \quad i = 1, \ldots, n \quad j = 1, \ldots, n \tag{6}$$

where:

- r is the distance between the middle point of each horizontal partition n of the external glass (points i) and the middle point of the horizontal partition n of the internal glass (points j).

- ϕ_i is the angle between the normal vector of each partition of the external glass i with respect to r for each partition j of the internal glass.

- ϕ_j is the angle between the normal vector of each partition of the internal glass j with respect to r for each partition i of the external glass.

- A_i is the area of the surface i.

Given the geometry of the problem it can be seen that $\phi_i = \phi_j$ and the areas are equal to Δz. Thus,

$$F_{ij} = \frac{\Delta z (\cos\phi_i)^2}{\pi r^2}.$$

Moreover, the form-factor can be explicitly expressed in terms of spatial dimensions. If defining the middle points $y_0 = (i - \frac{1}{2})\Delta z$ and $y_1 = (j - \frac{1}{2})\Delta z$, then $r = \sqrt{W^2 + (y_1 - y_0)^2}$ where W is the distance between the two sheets of glass. This results in $\cos\phi_i = \frac{W}{r}$ and finally:

$$F_{ij} = \frac{\Delta z (\cos\phi_i)^2}{\pi r^2} = \Delta z \frac{W^2}{\pi r^4}. \tag{7}$$

• J_i is the ratio of radiation energy that leaves the surface per unit area. It is defined in terms of the physical properties of the different types of glass: the emissivity (ε), the Stefan-Boltzman constant (σ) and the density (ρ) through the relation

$$J_i = \varepsilon_i \sigma T_i^4 + \rho_i G_i. \tag{8}$$

The wall cavity is defined as two parallel planes with a temperature gradient along these surfaces. By dividing each of these into n segments of equal length, as was done for the internal and external glass, it is assumed that each segment is an isothermal surface of the wall cavity, for a total of $2n$ surfaces.

For the calculation of the radiation heating transfer in the cavity surfaces it is necessary to apply the previous equation for each of the n partitions of the two sheets of glass.

The following equation details the amount of radiation heating exchange between each point i (for $i = 1, \ldots, n$) of the internal surface of the external glass and the internal surfaces $n + 1$ to $2n$ of the internal glass and viceversa.

$$
\begin{cases}
J_i = \varepsilon_i \sigma T_i^4 + (1 - \varepsilon_i) \sum_{j=n+1}^{2n} F_{ij} J_j, & i = 1, \ldots, n \\
J_i = \varepsilon_i \sigma T_i^4 + (1 - \varepsilon_i) \sum_{j=1}^{n} F_{ij} J_j, & i = n + 1, \ldots, 2n
\end{cases}
\tag{9}
$$

This linear system must then be solved with unknowns $\vec{x} = \{J_i\}_{i=1}^{2n} \in \mathbb{R}^{2n}$ which are expressed in compact form as:

$$
A\vec{x} = \vec{b}
$$

with $A \in \mathcal{M}_{2n \times 2n}, \vec{b} \in \mathbb{R}^{2n}$ given by,

$$
A = \left(\begin{array}{c|c} I & A_{1,2} \\ \hline A_{2,1} & I \end{array} \right), \quad \vec{b} = \{\varepsilon_i \sigma T_i^4\}_{i=1}^{2n}.
$$

The matrix $I \in \mathcal{M}_{n \times n}$ represents the identity matrix of dimension n and $A_{1,2} \in \mathcal{M}_{n \times n}, A_{2,1} \in \mathcal{M}_{n \times n}$ are defined as

$$
A_{1,2} = \begin{pmatrix}
(\varepsilon_1 - 1)F_{1,n+1} & (\varepsilon_1 - 1)F_{1,n+2} & \cdots & (\varepsilon_1 - 1)F_{1,j} & \cdots & (\varepsilon_1 - 1)F_{1,2n} \\
(\varepsilon_2 - 1)F_{2,n+1} & (\varepsilon_2 - 1)F_{2,n+2} & \cdots & (\varepsilon_2 - 1)F_{2,j} & \cdots & (\varepsilon_2 - 1)F_{2,2n} \\
\vdots & \vdots & \ddots & \vdots & \vdots & \\
(\varepsilon_i - 1)F_{i,n+1} & (\varepsilon_i - 1)F_{i,n+2} & \cdots & (\varepsilon_i - 1)F_{i,j} & \cdots & (\varepsilon_i - 1)F_{i,2n} \\
\vdots & \vdots & \vdots & \vdots & \ddots & \vdots \\
(\varepsilon_n - 1)F_{n,n+1} & (\varepsilon_n - 1)F_{n,n+2} & \cdots & (\varepsilon_n - 1)F_{n,j} & \cdots & (\varepsilon_n - 1)F_{n,2n}
\end{pmatrix},
$$

$$
A_{2,1} = \begin{pmatrix}
(\varepsilon_{n+1} - 1)F_{n+1,1} & (\varepsilon_{n+1} - 1)F_{n+1,2} & \cdots & (\varepsilon_{n+1} - 1)F_{n+1,j} & \cdots & (\varepsilon_{n+1} - 1)F_{n+1,n} \\
(\varepsilon_{n+2} - 1)F_{n+2,1} & (\varepsilon_{n+2} - 1)F_{n+2,2} & \cdots & (\varepsilon_{n+2} - 1)F_{n+2,j} & \cdots & (\varepsilon_{n+2} - 1)F_{n+2,n} \\
\vdots & \vdots & \ddots & \vdots & \vdots & \\
(\varepsilon_i - 1)F_{i,1} & (\varepsilon_i - 1)F_{i,2} & \cdots & (\varepsilon_i - 1)F_{i,j} & \cdots & (\varepsilon_i - 1)F_{i,n} \\
\vdots & \vdots & \vdots & \vdots & \ddots & \vdots \\
(\varepsilon_{2n} - 1)F_{2n,1} & (\varepsilon_{2n} - 1)F_{2n,2} & \cdots & (\varepsilon_{2n} - 1)F_{2n,j} & \cdots & (\varepsilon_{2n} - 1)F_{2n,n}
\end{pmatrix}.
$$

3. Numerical models

The numerical results of the models proposed previously are presented in this section. These models are first validated comparing them with the results obtained in Ismail et al. [17] and followed by the study carried out on the City of Refuge. The study specifically analyses temperature and total heat gain, q_{total}, defined as follows:

$$
\begin{aligned}
q_{total} &= \Delta x \sum_{j=1}^{n} U_{int}(T_{ind} - T_{ig}) + \Delta x U_c(T_f - T_{ig}) + \\
&+ \Delta x \sigma \varepsilon_{ig}(T_{ind}^4 - T_{ig}^4) + \alpha_{ig}\tau_{eg}I_o + Q_{ig}.
\end{aligned}
\tag{10}
$$

3.1. Testing prescriptive model

Firstly, the method proposed by Ismail et al. [17], is used to validate the numerical program, using the same values for the surrounding conditions and meteorological conditions. The characteristics of the prescriptive model of the glazed system used as a starting point are shown in Table 1.

Properties	External glass		Channel gap		Internal glass	
Thickness (m)	e_{eg}	0.007	e_c	0.003	e_{ig}	0.007
Emissivity	ξ_{eg}	0.08			ξ_{ig}	0.08
Absorptance	α_{eg}	0.06			α_{ig}	0.06
Transmission	τ_{eg}	0.86			τ_{ig}	0.86
Density(kg/m^3)	ρ_{eg}	2500	ρ_f	1293	ρ_{ig}	2500
Specific heat(Jkg/K)	c_{eg}	750	c_f	1004	c_{ig}	750
Thermal	$R_{se} + R_{eg}$		R_f		$R_{si} + R_{ig}$	
resistivity $(m\,K/W)$	0.04 + 0.0025		0.125		0.0025+0.18	

Table 1: Prescriptive model characteristics.

Following the description of the characteristics of the prescriptive model the results featured in the following graphs for heat transfer (q_{total}) and evolution of temperature in the interior glass surface at mid height (T_{igzmed}) are assessed. When compared with the results obtained by Ismail et al. [17], the numerical solution of this model first shows that the behaviour in the graphs is the same, and secondly, that the values obtained coincide with those of the prescriptive model (Figure 6).

3.2. Proposed model applied to the City of Refuge

The case study is geometrically defined following the plans obtained from the Le Corbusier Foundation. The final construction plans of the City of Refuge, from September 1933, were used
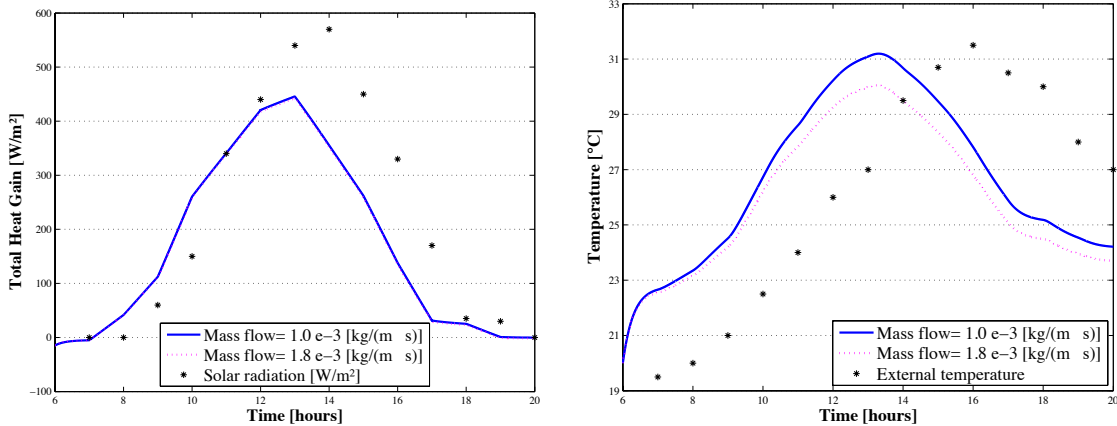
(a) Variation of total heat gain q_{total} over time.

(b) Effect of air mass flow on the temperature of glass interior surface T_{igzmed} over time.

Figure 6: Testing prescriptive model.

in surveys for each of the levels in order to obtain a better understanding of the building and to choose the room for study: the women's dormitory on the first floor, to the left of the staircases (Figure 2), which had the greatest surface area, 295 m^2, the longest length of *mur neutralisant*, 37.2 m, and highest occupancy, 67 beds.

The surrounding conditions imposed in the two-dimensional model (see Section 2.1) correspond to each of the enclosures defined in Figure 7, in a horizontal section carried out at a height of 2.35 m, at a level with the impulse grid for air ventilation.

Three types of *mur neutralisant* were proposed and tested by Saint Gobain in August 1932 [19], with measurements 2+100+2, 7+100+7 and 12+100+12 mm. This allowed a precise and rigorous assessment of the true conditions under which the *mur neutralisant* system might have operated, had it been incorporated, bearing in mind that Le Corbusier reserved a space for the possible incorporation into the wall of 7+100+7 mm glazing at a later stage. We perform the numerical simulation of this type of glass chosen by Le Corbusier.

Figure 4 shows the properties of the physical phenomena for the specific *mur neutralisant* system simulated, including the percentages of solar radiation transmitted through the *mur neutralisant*. All the values for emissivity, absorptance, transmission, density, specific heat and thermal resistance of glazing have been taken from the data provided by Saint Gobain [23], Table 2.

The value of $T_{ig1d(m)}$, which is the temperature of the glazed enclosure, is imposed on boundary Γ_1. This value is obtained from the result of the 1D problem which simulates the evolution of temperatures in the *mur neutralisant*. The radiant temperature of the interior enclosures of the

Properties	External glass		Channel gap		Internal glass	
Thickness (m)	e_{eg}	0.007	e_c	0.10	e_{ig}	0.007
Emissivity	ξ_{eg}	0.07			ξ_{ig}	0.07
Absorptance	α_{eg}	0.14			α_{ig}	0.14
Transmission	τ_{eg}	0.79			τ_{ig}	0.79
Density (kg/m^3)	ρ_{eg}	2500	ρ_f	1293	ρ_{ig}	2500
Specific heat $(kg\,J/K)$	c_{eg}	750	c_f	1004	c_{ig}	750
Thermal	R_{eg}		R_f		R_{ig}	
resistivity $(m\,K/W)$	0.17545		0.125		0.17545	

Table 2: Properties of simulation hypothesis 7+100+7 mm.

room studied is imposed on boundaries Γ_2, Γ_4, Γ_5, Γ_6, Γ_7 y Γ_8 (see Figure 7). T_{extef} is imposed on boundary Γ_3. This corresponds to the point where the flow for the *respiration exacte* is boosted. T_{op} is the initial operative temperature in the room studied over the space Ω.

The source term due to the occupancy, involved in the evolution of the temperature in the room (equation (1)) for the 2D problem, is calculated according to a ratio of 25 $person/m^2$ and an energy charge of 46 $W/person$. This is defined as follows:

$$\varphi = \frac{0.25\frac{person}{m^2} \cdot 46\frac{W}{person}}{\rho c_f H} = 0.00316\frac{K}{s} \tag{11}$$

where ρ is the air density (kg/m^3), c_f the specific heat of the air $(kg\,J/K)$ and H the height of the room (m).

Initial radiant temperature conditions obtained from the simulations with the DesignBuilder energy simulation tool have only been used as a starting point for the initial radiant temperature conditions of the room studied. See Appendix A for details.
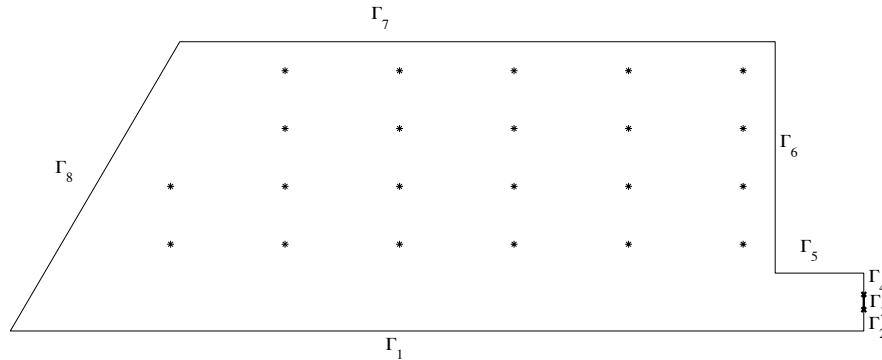

Figure 7: Labels corresponding to each of the surrounding conditions of the room studied and probes of internal points where the temperature is measured (marked with asterisks).

3.2.1. Initial conditions

In this subsection we specify the initial conditions for the problem. The numerical simulations are developed for two representative days in winter and summer, namely, August 15 and December 30. The calculations are made referring to solar time. The total time of the numerical simulation is two solar days (48 h) and the initial data specified here refers to the first solar time hour.

- *Initial climate conditions*

The climate files for Paris Orly were used, considering exactly the same files used by Design-Builder. See Appendix A.

- *Initial temperatures and impulse flow in the mur neutralisant (1D problem)*

As was mentioned above, for the initial temperature conditions a previous calculation was performed using the simulations of DesingBuilder, based on the EnergyPlus simulation tool. The resulting data gives an initial temperature in the interior of the room of 27.58°C for summer and 7.14°C for winter. The initial temperatures for the internal glass and the temperature of the room are the same, so $T_{int} = T_{igini} = 27.58$°C in summer and $T_{int} = T_{igini} = 7.14$°C in winter. The external glass is supposed to be at the same exterior temperature, so $T_{egini} = 19.7$°C in summer and $T_{egini} = -3.8$°C in winter.

In order to establish the impulse temperature of the active chamber, a 10°C thermal leap was considered in relation to the temperature of the desired indoor temperature of the room: 20°C in winter and 25°C in summer. Therefore, the constant impulse temperatures in the active chamber are set to 30°C in winter and 15°C in summer.

The Saint Gobain technicians had established that high flows (120 l/s and 150 l/s) increased energy losses as a result of the turbulence inside the active chamber, with a decrease in the heat exchange between fluid and glass surfaces. A more appropriate 60 l/s flow was chosen for the air impulse flow into the active chamber. To introduce this data into the `FreeFem++` code, it is necessary to relate this flow to the mass flow which is the quantity that is really imposed. Thus, we calculate the mass flow η to be imposed as follows:

$$\eta = \rho \cdot v = \frac{\rho \cdot q}{S} = \frac{1.293 \frac{kg}{m^3} \cdot 60 \frac{l}{s} \cdot \frac{1 \ m^3}{1000 \ l}}{0.10 \ m \cdot L} = 0.7758 \frac{kg}{s \cdot m \cdot L} \tag{12}$$

where ρ is the air density (kg/m^3), v the velocity (m/s), q the impulse flow (m^3/s), and S the surface area of the passage section where the *respiration exacte* is implemented (m^2). Note that this quantity is normalised with a characteristic length L associated to the dimension of the 3D

case which is avoided in the 2D calculation ($L = 1$ in simulations).

- *Initial temperatures and impulse flow in the room (2D problem)*

The impulse temperature at the *respiration exacte* is fixed at 20°C in winter and 25°C in summer. These are the desired indoor temperatures stated in the tests carried out by Saint Gobain. The initial temperature conditions in the interior of the room have already been specified, 7.14°C for winter and 27.58°C for summer.

3.2.2. 1D model results

First, we study the evolution of the temperatures in the *mur neutralisant*, by considering a constant temperature in the room. The objective is to study the influence of the external temperature, radiation and the temperature of the air impulsed between the glass, on the temperature of the internal glass. Therefore, for the first test it is enough to consider the numerical simulation produced with the 1D code described in Subsection 2.2.2.

- **Evolution of heat transfer**

First, we study the relation of the heat transfer (q_{total}) in the *mur neutralisant* to the solar radiation.

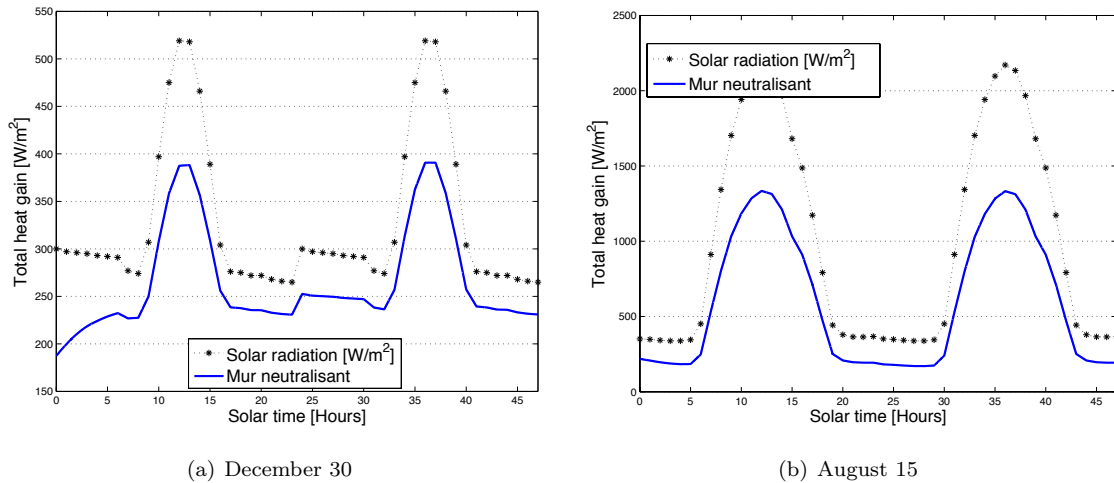(a) December 30   (b) August 15

Figure 8: Total heat gain in the *mur neutralisant* for the two days under study.

Figure 8 represents the evolution over time of the total heat gain together with the solar radiation for both cases. In the case of the summer day (Figure 8(b)), the maximum heat transfer

19

difference occurs at 12:00 h each day when there is 2200 W/m^2 solar radiation in the exterior. Heat transfer to the interior atmosphere for 7 mm glass manages to transfer 63.3% which does not seem to high to provide reasonable temperature to the interior to achieve comfort conditions.

In contrast, this heat gain increases to 79.2% for the winter sample (Figure 8(a)) where the maximum heat transfer to the interior is required. For the day studied, the maximum solar radiation received is 535 W/m^2 also around midday. The most positive point of this case is that even after 15:00 h the heat gain remains quite high demonstrating the advantages of the *mur neutralisant* system.

● **Evolution of the temperature of the internal glass**

Figure 9 shows the evolution over time of the temperature of the internal glass together with the exterior temperature.
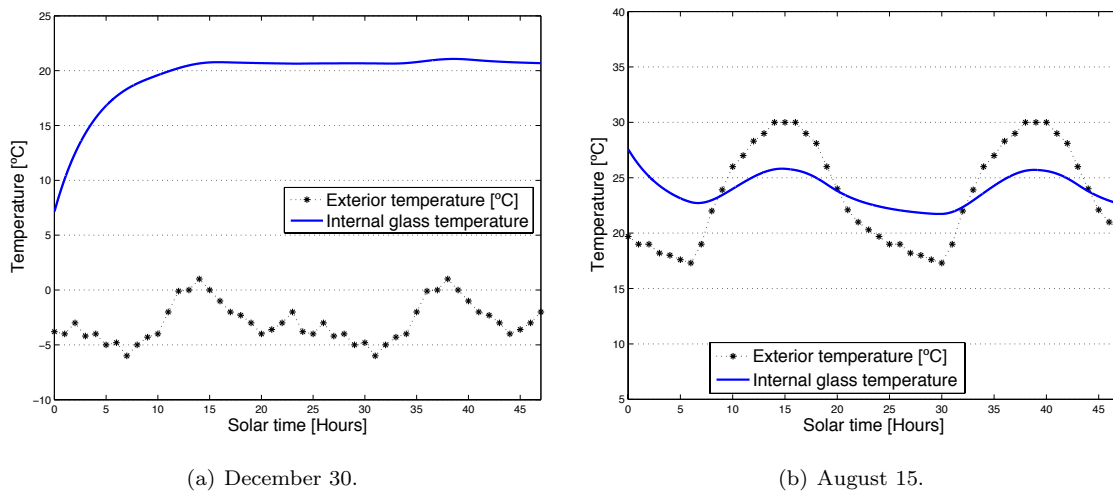

(a) December 30.

(b) August 15.

Figure 9: Evolution of the temperature of the internal glass surface for the two days under study.

For the winter case (Figure 9(a)), the temperature of the interior glass achieved remains almost constant, at approximately 20.7°C. With a small increase of temperature, following the increase of the external temperature, it goes up to 21.2°C. The strong increase in the first 12 hours approximately is due to the initial condition. After this time, the temperature is established and there is no influence from the initial data.

In summer (Figure 9(b)), the behaviour of the *mur neutralisant* manages to reduce the temperature in the interior glass in a range of 21.7°C - 25.7°C once established. Observe that the temperature of the internal glass buffers the exterior temperature in the hottest hours, achieving

a difference of 4°C less.

3.2.3. Coupled 1D/2D model results

In this section we show the results of the coupled model, taking into account: solar radiation, external temperature, temperature of the impulsed air in the *mur neutralisant* and the temperature of the impulsed air in the room. We analyse the results obtained for the temperature inside the *mur neutralisant* and the temperature in the room. We have studied two scenarios, with or without occupancy defined by equation (11) in the room. In the case considered, the schedule of occupancy was fixed between 18:00 h and 8:00 h each day.
To be brief, we do not show the graphics corresponding to the 1D results here because the behaviour of the *mur neutralisant* has already been shown.

• **Evolution of temperature in the room**

Before analysing the results for the interior temperatures of the room it is important to note two specific aspects relating to the general behaviour of the area occupied:
- In the southwest corner, the accumulation of air that is less cold than in the rest of the room in winter and less hot in summer provides a suitable temperature in the area that is farthest away from the air impulse, also encouraging air convection to the area with greatest occupancy.
- In contrast, in the northeast corner in winter there are colder air currents, while in the summer the currents are hotter. Although this is considered one of the least favourable areas in the room, this is not entirely relevant as this corner is actually a small room.

Figures 10 and 11 show the isovalues of the temperature obtained for the representative hour 25 (at the middle of the first occupation range) for both cases in winter and summer. We comment on these below:

Winter after 25 hours (Figure 10):
In this case the temperature of the active chamber is maintained constant at 30 °C and the *respiration exacte* impulse temperature occurs at 20 °C. Thus, the temperature of the room with occupancy increases by 3.5 °C with respect to the air impulse by *respiration exacte*, while in the case without occupancy the increase is 2 °C. We can see how the increase in temperature when occupied occurs in an almost regular way throughout the room, always with higher temperatures near the *mur neutralisant* than in the rest of the room.

Summer after 25 hours (Figure 11):

When the active chamber temperature is maintained constant at 15 °C and the *respiration exacte* occurs at 25 °C in neutral air conditions, the temperature in the room for the occupancy case increases by only 1.5 °C with respect to the temperature supplied by *respiration exacte*. While if there is no occupancy, the temperature undergoes a steady increase of 0.5 °C. We observe the same behaviour as in the winter case, the temperature increases uniformly in the room when it is occupied.

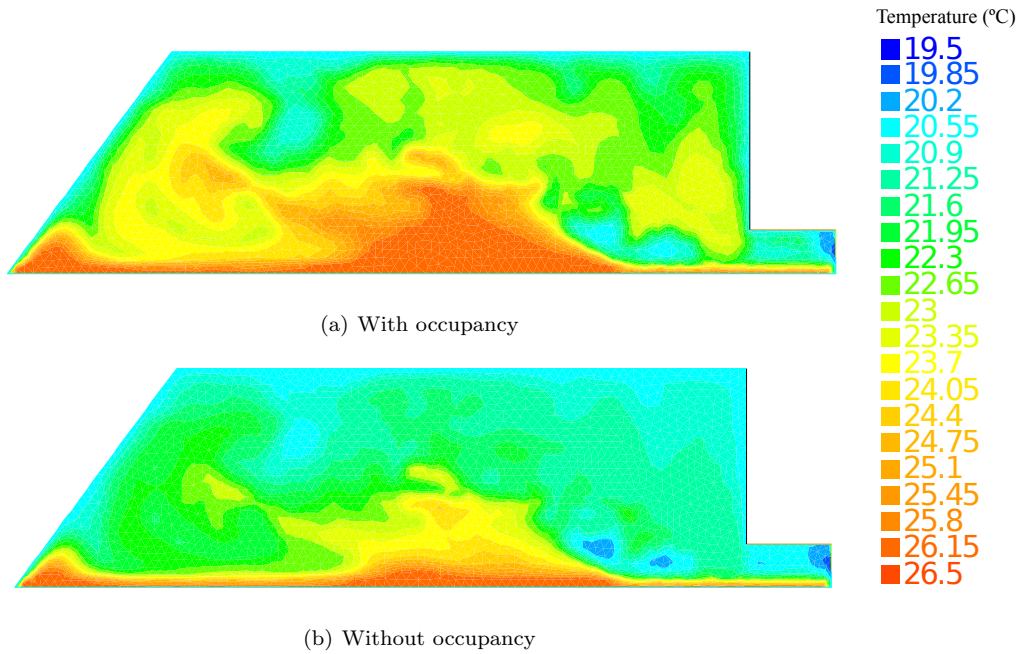(a) With occupancy

(b) Without occupancy

Figure 10: Simulation at the middle of the pane height for December 30, after 25 hours, (with *respiration exacte* temperature at 20 °C and *mur neutralisant* temperature at 30 °C).

To show the results more clearly we have measured the temperature obtained by the simulation in several points located in the room, marked in Figure 7. We then averaged these values to obtain an averaged temperature inside the room for each time. The results are shown for the 48 hours of simulation in Figure 12 and for clarity, we have marked the ranges of hours when occupancy is considered. The temperature is more stable if the occupancy load is not taken into account. For winter and summer cases, the temperatures remain similar even after the first occupancy range, and a clear increase in temperature is observed during the occupancy hours.

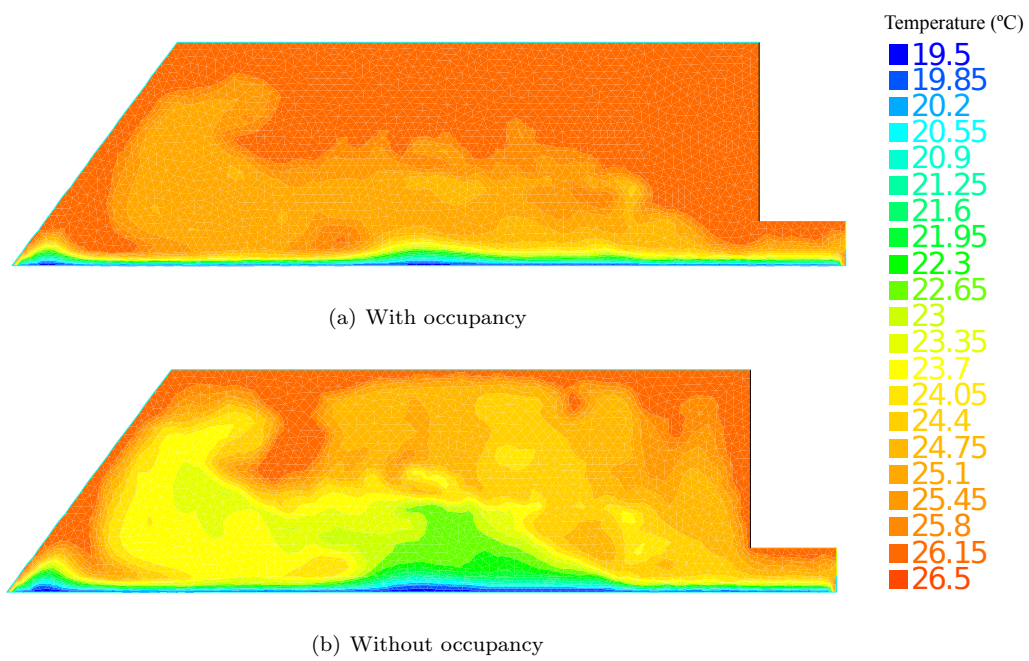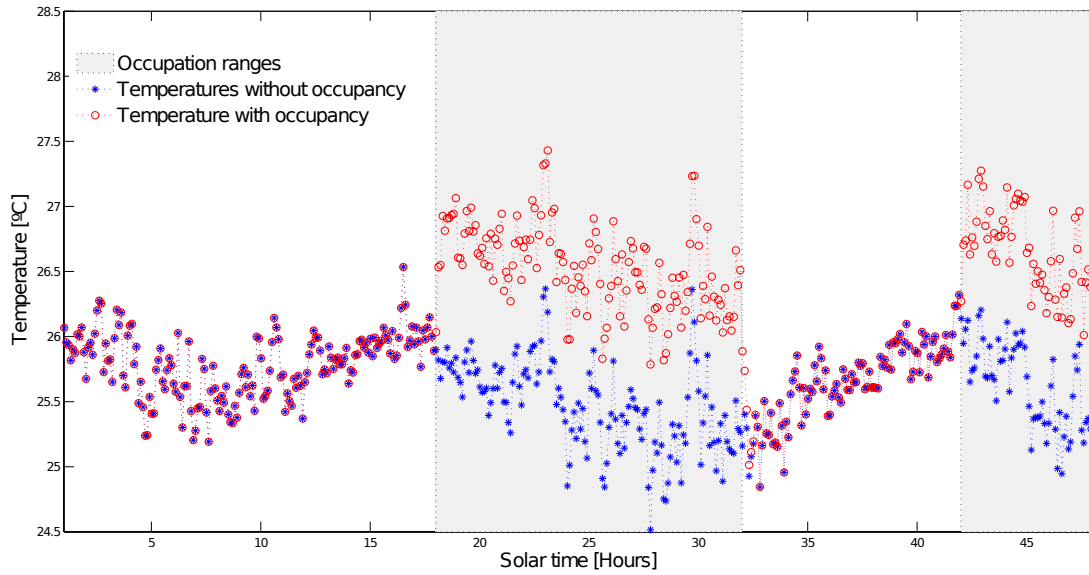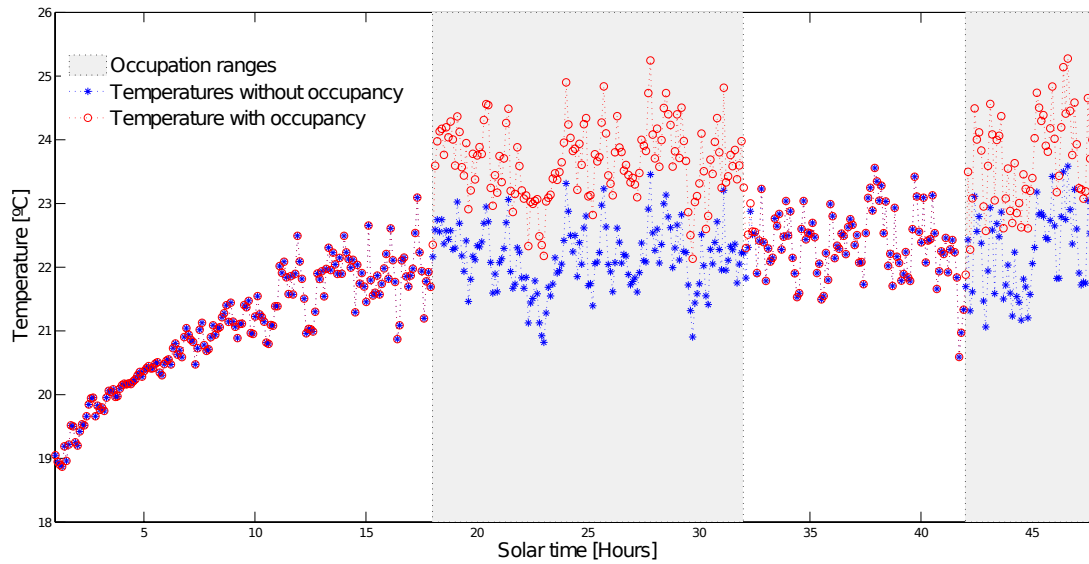(a) With occupancy

(b) Without occupancy

Figure 11: Simulation at the middle of the pane height for August 15, after 25 hours, (with *respiration exacte* temperature at 25 °C and *mur neutralisant* temperature at 15 °C).

(a) August 15.

(b) December 30.

Figure 12: Comparison of the temperature in the room with and without occupancy load.

24

4. Conclusions

The `FreeFem++` simulations and their subsequent analysis support Le Corbusier's proposal to combine the *mur neutralisant* and *respiration exacte* for the environmental conditioning of the City of Refuge, G. Lyon's calculations for both systems and the main conclusions reached by J. Le Braz in the St. Gobain tests. This shows the importance of this proposal, more than 50 years ahead of its time in relation to modern active façade systems, of which Le Corbusier's project is the clearest precursor.

In the results we observe uniform room temperature and suitable climate conditions for both winter and summer cases. There is an exception at the Northeast corner and mainly at the Southwest corner due to the irregular geometry of the room. The thermal activity in the *mur neutralisant* balances the external temperature to produce a milder temperature of the internal glass and in turn, approach climate comfort conditions within the room.

In winter for an air flow supply (*respiration exacte*) of 20°C and a chamber temperature of 30°C (heating), the superficial temperature of the internal glass is uniform with slight variations between 20.7°C and 21.2°C. The temperature in the room for the representative solar hour 25 (at the middle of the first occupation range) and an exterior temperature of -4°C is homogeneous with average values of 23.5°C if occupied and of 22°C if not.

Similarly for the summer case, for an air flow supply (*respiration exacte*) of 25°C (neutral primary air) and an air flow supply of 15°C (into the active chamber), climate comfort is maintained. The highest exterior thermal oscillation leads to a range of internal glass temperature between 21.7°C and 25.7°C. In addition, the temperature of the room for the solar hour 25 −the most unfavourable case because of night occupancy− is 25.5°C with the room empty and presents a small increase to 26.5°C when occupied.

The innovative technologies developed by Le Corbusier based on the *mur neutralisant* and the *respiration exacte*, provide a new conditioning system through the building envelope ahead of the first air conditioning systems then appearing in the United States. Unlike these, Le Corbusier proposed to provide the façade with heating and air-conditioning of the interior spaces and a ventilation mechanism through the *respiration exacte*. He was clearly the precursor of the later active system façades.
Thus, comfort conditions and thermal uniformity are achieved by simply heating or cooling the air volume inside the *mur neutralisant*, by at most 10°C −for the most unfavourable conditions− in relation to the desired temperature into the room. In theory this system seems more economical

than the use of a standard air conditioning machine to heat or cool the total mass of air in the room.

However, to really value the efficiency of the system developed by Le Corbusier, a more extensive study should be carried out, especially focusing on the comparison with alternative conditioning systems. Given that no cooling system was included in the building and the traditional heating system had to be installed, these kinds of comparisons entail major difficulty as there is no data for comparison.

Acknowledgements

Appendix A. Initial conditions

For the calculation with `FreeFem++` an energy model generated and assessed with Design-Builder was produced in order to execute a simulation of the environmental conditions of the room studied. This was done following the room's real construction, with a single glazed façade, as the *mur neutralisant* could not finally be built with double glazing. In turn this made it possible to apply both Le Corbusier's proposed innovations to real conditions. The DesignBuilder simulation followed two different procedures allowed by the program. The first obtains a global assessment of the environmental conditions in the room using EnergyPlus [7], while a second more advanced procedure provides an assessment of these environmental conditions at each point in the room using CFD algorithms. We collect in Table A1 the climatic conditions for the city of Paris including the main data of the climate file considered for the calculation.

The specific calculation conditions for both procedures are as follows:

Specific conditions for the EnergyPlus calculation

• *Solar protection*

The type of solar protection used consists of a system with 10 mm thick vertical PVC slats with a conductivity equal to 0.16 W/mK. The type of shade has been placed 70 mm back from the façade.

It should be noted that this study was carried out from a thermal perspective, and therefore, aspects characteristic of natural daylight were not taken into account when programming the solar protection system.

Month	Dry-Bulb temp. °C	Relative humidity %	Infrared horiz. rad. Wh/m^2	Normal rad. Wh/m^2	Sky rad. Wh/m^2	Global horiz. rad. Wh/m^2	Direct normal rad. Wh/m^2	Diffuse horiz. rad. Wh/m^2
January	3.87	91.4	115.31	1415.06	286.93	32.37	31.25	22.84
Febrary	4.15	68.1	178.67	1404.02	283.67	58.08	49.52	38.29
March	7.00	75.5	272.13	1383.50	298.59	95.21	46.03	71.35
April	9.98	72.8	374.35	1358.62	308.70	151.45	72.35	104.07
May	14.33	66.4	447.44	1338.44	330.57	192.22	89.41	130.72
June	16.83	77.8	482.3	1325.71	349.51	221.60	123.60	133.98
July	19.44	65.3	465.57	1324.33	357.76	223.44	140.79	125.68
August	19.69	68.1	402.79	1334.50	358.15	202.94	154.68	103.73
September	15.76	77.8	311.96	1353.81	341.69	130.05	84.78	84.06
October	11.36	81.4	213.75	1377.76	316.40	84.73	74.24	51.10
November	6.48	89.3	134.68	1399.88	299.06	43.47	43.90	29.07
December	4.51	89.7	98.22	1414.06	290.27	25.33	18.43	20.34

Table A1: Monthly average of the most representative parameters of Energy Plus Weather (EPW) file of Paris.

• *Adjacencies*

The spaces adjacent to the room studied were taken into account in the construction of the model. Spaces with the same operative and use conditions as the room under study have been defined as adiabatic. However, uninhabitable spaces and common areas have been considered to be zero occupancy areas. Figure A1 shows the model with the room under study highlighted in red.
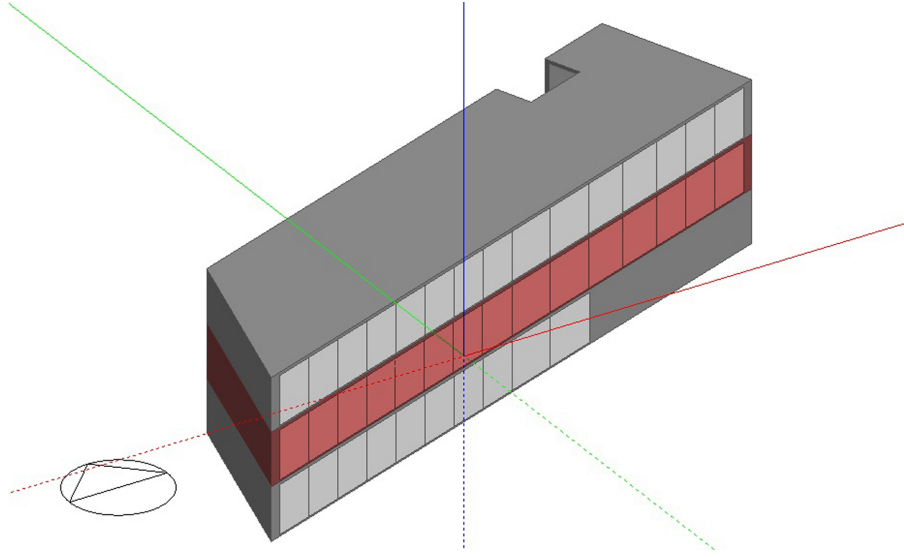
Figure A1: Adjacencies considered in the model of the room under study.

- *Infiltrations*

Different infiltration values were introduced into the model depending on the intended use of each of the spaces. Table A2 shows the infiltration flows considered in each of the areas of the floor studied.

As can be observed, infiltrations were not considered in the room under study as the mechanical ventilation system (*respiration exacte*) maintains it at a high pressure in relation to the exterior. Therefore, the amount of uncontrolled air introduced through the glazed façade is considered negligible.

- *Ventilation systems*

In large rooms this system allowed 1 ACH in winter and 2-3.5 ACH in summer. Therefore air flow impulse was set at 300 m^3/h and 1050 m^3/h for winter and summer respectively.

It was observed that a 525 x 225 mm mesh has an actual surface of $0.118m^2$ and an effective surface of $0.101m^2$, so with these summer and winter impulse flows the following passage speeds would result:

$$
\begin{cases}
v_{winter} = \frac{300 \ m^3/h}{(0.098 \ m^2 \cdot 0.85)} \cdot \frac{1 \ h}{3600 \ s} = 1 \ m/s \\
\\
v_{summer} = \frac{1050 \ m^3/h}{0.098 \ m^2 \cdot 0.85)} \cdot \frac{1 \ h}{3600 \ s} = 3.5 \ m/s
\end{cases}
\tag{A2}
$$

Spaces	Surface of floor	Surface exposed to outside		Infiltrations renovations/h
		Opaque	Glazed	
Study room	297.67 m^2	136.20 m^2	118.50 m^2	0
Attached room	7.12 m^2	14.76 m^2	3.00 m^2	0.2
Common area	48.63 m^2	17.39 m^2	6.95 m^2	3
Toilets	23.05 m^2	14.24 m^2	6.00 m^2	1
Lifts	4.75 m^2	0 m^2	0 m^2	1

Table A2: Types of infiltration.

Specific conditions for the calculations of CFD

• *Flow equilibrium*

The model's incoming and outgoing flows must be balanced in order to ensure the mass balance in simulations using CFD. Admittance flows are introduced through the impulse mesh: 291.66 l/s in summer and 83.33 l/s in winter. Extraction flows take place through a small opening below the entry door to the room under study.

• *Temperatures*

Temperature data was obtained from the simulation results with EnergyPlus in DesignBuilder. Table A3 reflects the radiant temperatures imported into the CFD calculation model for each type of enclosure, (see numbering in Figure A2), for every day and hour simulated.
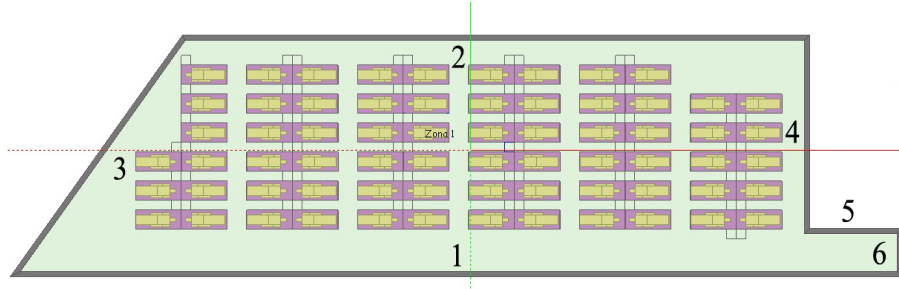
Figure A2: Numbering of individual energy model enclosures for the purposes of correspondence with radiant temperatures.

Type of wall		Surface (m^2)	Radiant temperatures (^oC) December 30		August 15	
1	South wall façade	11.77	16.00	16.37	27.33	28.97
1	South glass façade	118.50	13.97	13.65	42.72	22.55
2	North wall	80.50	21.12	17.50	28.63	27.14
3	West wall	43.45	21.00	17.53	28.59	27.57
4	Interior partition insulated a	38.50	21.19	17.54	27.65	27.20
5	Interior partition insulated b	13.50	18.99	17.10	27.71	27.18
6	Interior partition not insulated	6.60	18.79	15.30	30.19	27.44
6	Door	297.67	4.16	1.58	29.97	25.86
7	Ceiling	297.67	22.21	20.50	27.64	27.06
8	Floor	297.67	25.37	21.55	27.13	26.81

Table A3: Radiant temperature of each type of wall according to numbering.

- *Meshing*

The CFD internal analysis field was established based on the generation of a mesh defined using two factors: the predetermined spacing of the mesh (0.1 m) and the tolerance in the overlapping of mesh lines (0.01 m). It is important to establish different densities, since certain areas in the room under study require more precision than others, as is the case of the entry partition with the impulse grid into the room and the door opening for extraction, making finer meshing advisable in this area.

- *Convergence*

The calculations carried out were simulated following the $K-\epsilon$ "Standard", one of the most widely used turbulence models, using transport equations with turbulent flow properties: convection and diffusion of turbulent energy. K represents the turbulent kinetic energy transported while ϵ is the

turbulent dissipation transported.

A maximum number of iterations and acceptable residual values for mass, velocity, temperature and turbulence were established. Once these requirements were met the results obtained could be considered valid. In the computations developed here, we established a maximum of 10000 iterations and a residual value of 10e-6 to ensure the convergence. We show in Figure A3 the convergence graphic displayed by DesignBuilder where the normalized residuals are represented in front of the number of iterations.
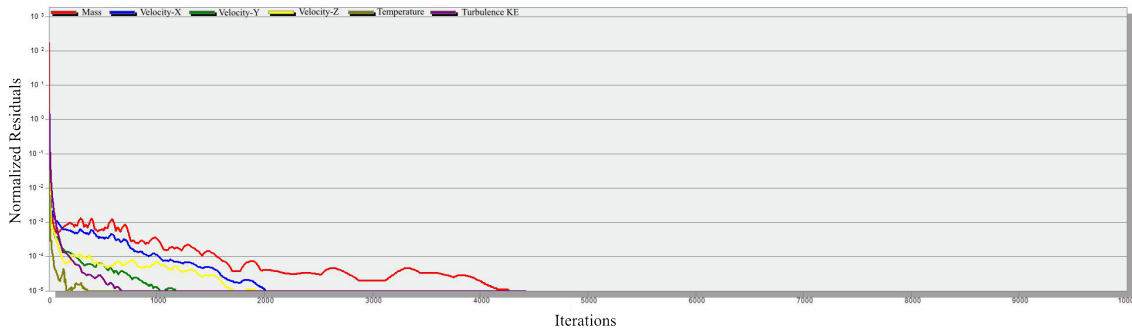

Figure A3: Normalized residual values versus iterations

Appendix B. Nomenclature

ρ	Density of glass $[\frac{kg}{m^3}]$
c	Specific heat $[\frac{J}{kgK}] = [\frac{Ws}{kgK}]$
V	Area $[m^2]$
η	Mass flow in the channel per unit depth $[\frac{kg}{sm}]$
σ	Stephan-Boltzman constant $5.57 10^{-8}$
ε_{eg}	Emissivity of external glass
ε_{ig}	Emissivity of internal glass
α_{eg}	Absorbency of external glass
α_{ig}	Absorbency of internal glass
τ_{eg}	Energy transmission of external glass
τ_{ig}	Energy transmission of internal glass
Q_{ig}	Net radiant heat transfer in the internal glass
Q_{eg}	Net radiant heat transfer in the external glass
U	Transmittance coefficient $[\frac{W}{m^2K}]$
U_{ext}	Transmittance coefficient of external glass $[\frac{W}{m^2K}]$ $$U_{ext} = \frac{1}{R_{se} + R_{eg} + R_{si}}$$
U_{int}	Transmittance coefficient of internal glass $[\frac{W}{m^2K}]$ $$U_{int} = \frac{1}{R_{se} + R_{ig} + R_{si}}$$
R_{se}	Film exterior coefficient $[\frac{m^2K}{W}]$
R_c	Thermal resistance of channel $[\frac{m^2K}{W}]$
R_{si}	Film interior coefficient $[\frac{m^2K}{W}]$
R_{eg}	Thermal resistance of external glass $[\frac{m^2K}{W}]$ $$R_{eg} = \frac{e_{eg}}{\lambda_{eg}}$$
R_{ig}	Thermal resistance of internal glass $[\frac{m^2K}{W}]$ $$R_{ig} = \frac{e_{ig}}{\lambda_{ig}}$$
e_{eg}	Depth of external glass $[m]$
e_{ig}	Depth of internal glass r $[m]$
λ_{eg}	Thermal conductivity of external glass $[\frac{W}{mK}]$
λ_{ig}	Thermal conductivity of internal glass $[\frac{W}{mK}]$

[1] Balacco, C., Colombar, M. Thermal behaviour of interactive mechanically ventilated double glazed façade: bib-dimensional analysis. Energy and Buildings 38 (2006) 1-7.

[2] Balocco, C. A non-dimensional analysis of a ventilated double façade energy performance. Energy and Buildings 36 (2004) 35-40.

[3] Boesiger, W. *Le Corbusier et Pierre Jeanneret: oeuvre complete. Vol 2, 1929-1934* (1999). Basel, Switzerland: Birkhauser.

[4] Brandl, D., Mach, T., Grobbauer, M., Hochenauer, C. Analysis of ventilation effects and the thermal behaviour of multifunctional façade elements with 3D CFD models. Energy and Buildings (2014), http://dx.doi.org/10.1016/j.enbuild.2014.09.036.

[5] Chen, YH., Sa, Sz., Zhou, Ys., Wei, S.X., Tan, Z.H. A mathematical model of thermal channel glazing curtain wall. Building Energy & Environment 25 (2006) 10-5.

[6] DesignBuilder v.2.4.2.026. [Online], Available: http://www.designbuilder.es/descargas/ software-designbuilder [17 June 2013].

[7] EnergyPlus v.6.0. U.S. Department of Energy (DOE). [Online], Available: http://apps1.eere.energy.gov/buildings/energyplus/energyplus_training.cfm [2 September 2013].

[8] Faggembauu, D., Costa, M., Soria, M., Olivia, A. Numerical analysis of the thermal behaviour of ventilated glazed façades in Mediterranean climates. Part I. Development and validation of a numerical model. Solar Energy 75 (2003) 217-28.

[9] Fernandez, V., Gallo, E. La Cité de Refuge de Le Corbusier, une étude menée sur la demande de François Chatillon, ACMH. Séminaire Efficacité énergétique. [Online], Available: http://www.futursurbains.fr/fichiers/S%202013.pdf [13 May 2013].

[10] FreeFem++ v.-3.20. [Online], Available: http://www.FreeFem.org/ff++/ [30 October 2011].

[11] Fondation of Le Corbusier. [Online], Available: http://www.fondationlecorbusier.fr. [7 January 2012].

[12] Gallo, E., Fernandez, V. *A factory for well-being, innovation in the heating system and the curtain-wall in Le Corbusier's Salvation Army City of Refuge, Paris 1933.* (2010) Toulouse: CDHTE-CNAM, Ecole Nationale d'Architecture.

[13] Ghadimi, M., Ghadamian, H., Hamidi, A.A., Shakouri, M., Ghahremanian, S. Numerical analysis and parametric study of the thermal behavior in multiple-skin façades. Energy and Buildings 67 (2013) 44-55.

[14] Hecht, F. New development in freefem++. J. Numer. Math. 20 (2012), no. 3-4, 251-265. 65Y15.

[15] Ismail, K.A.R., Henríquez, J.R. Modeling and simulation of a simple glass window. Solar Energy Materials & Solar Cells 80 (2003) 355-374.

[16] Ismail, K.A.R., Henríquez, J.R. Two-dimensional model for the double glass naturally ventilated window. International Journal of Heat and Mass Transfer 48 (2005) 461-475.

[17] Ismail, K.A.R., Henríquez, J.R. Simplified model for a ventilated glass window under forced air flow conditions. Applied Thermal Engineering 26 (2006) 295-302.

[18] Joe, J., Choi, W., Kwak, Y., Huh, J-H. Optimal design of a multi-story double skin façade. Energy and Buildings 76 (2014) 143-150.

[19] Le Braz, J. La transmission de la chaleur gràve à travers le verre: Des idées nouvelles sur le chauffage des habitations. Glaces et Verres 20 (1933) 12-18.

[20] Liu, M., Bjarne Wittchen, K., Kvols Heiselberg, P., Vildbrad Winther, F. Development and sensitivity study of a simplified and dynamic method for double glazing facade and verified by a full-scale façade element. Energy and Buildings 68 (2014) 432-443.

[21] Oliveti, G., Arcuri, N., Bruno, R., De Simone, M. An accurate calculation model of solar heat gain through glazed surfaces. Energy and Buildings 43 (2011) 269-264.

[22] R.L. La maison de verre de MM. Le Corbusier et Jeanneret et le mur neutralisant. Glaces et Verres 20 (1933) 10-12.

[23] Saint Gobain, [Online], Available: http://www.saint-gobain-sekurit.com/SP/index.asp?nav1=AU&nav2=AUSM/ [13 September 2012].

[24] Shameri, M.A., Alghoul, K., Sopian, M., Fauzi M., Sain, Elayeb, O. Perspectives of double skin façade systems in buildings and energy saving. Renewable and Sustainable Energy Reviews 15 (2011) 1468-1475.

[25] Taylor, B. Technology, society, and social control in Le Corbusier's Cité de Refuge, Paris 1933. Oppositions 16 (1979)168-185.

[26] Zanghirella, F., Perino, M., Serra, V. A numerical model to evaluate the thermal behaviour of active transparent façades. Energy and Buildings 43 (2011) 1123-1138.

[27] Zhou, J., Chen, Y. A review on applying ventilated double-skin façade to buildings in hot-summer and cold-winter zone in China. Renewable and Sustainable Energy Reviews 14 (2010) 1321-1328.